An image analysis method to study the relationship between seagrasses and their epiphytes

Chi Huang

chuang2@islander.tamucc.edu

Texas A&M University-Corpus Christi https://orcid.org/0000-0002-4078-3463

Mehrube Mehrubeoglu

Texas A&M University-Corpus Christi

Carissa Piñón

Texas A&M University-Corpus Christi

Kirk Cammarata

Texas A&M University-Corpus Christi

Research Article

Keywords: Epiphyte, Image analysis, Seagrass, Seagrass epiphyte relationship, Algae, Biofilm, Environmental conditions, Biomass ratio, Leaf coverage, Community composition

Posted Date: July 22nd, 2024

DOI: https://doi.org/10.21203/rs.3.rs-4645103/v1

Version of Record: A version of this preprint was published at Marine Biology on December 30th, 2024. See the published version at https://doi.org/10.1007/s00227-024-04577-1.

Declaration Conflict of Interest

Declaration of interests

☒The authors declare that they have no known competing financial interests or personal relationships that could have appeared to influence the work reported in this paper.

☐The authors declare the following financial interests/personal relationships which may be considered as potential competing interests:

An image analysis method to study the relationship between seagrasses and their epiphytes

Authors: Chi Huang [a], Mehrube Mehrubeoglu [b], Carissa Piñón [a], Kirk Cammarata [a, *]

[a] Department of Life Science, Texas A&M University-Corpus Christi, TX 78412, USA

[b] Department of Engineering, Texas A&M University-Corpus Christi, TX 78412, USA

[*]Corresponding author

Abstract:

Seagrasses are globally threatened due to increasing environmental stressors in coastal ecosystems. Excessive accumulation of algal epiphytes is suggested to be harmful to seagrasses, but an understanding of the quantitative relationship between epiphyte accumulation and effects on seagrass is still incomplete. The biomass, pigment and morphological measures widely used in understanding seagrass-epiphyte relationships provide limited spatiotemporal resolution of the dynamics of epiphyte colonization relative to host leaf growth and senescence. In this study, color scanning and image analysis methods were developed and validated to characterize epiphyte accumulation relative to seagrass host morphology. *Thalassia testudinum* collected monthly or bimonthly from July 2019 to April 2020 in Redfish Bay, Texas, was analyzed through traditional and image-based measures. Spectral Angle Mapper (SAM) algorithms within the ENVI Program distinguished the pixels of many epiphytes collectively from epiphyte-free leaf areas based on RGB color bands. Misclassified pixels were < 10% in 94% of the analyzed images. Classification accuracy was also evaluated by correlation of traditional biomass and morphology metrics vs. image-based metrics for more than 2,000 seagrass and

epiphyte images collected across different seasons and environmental conditions. Image-derived seagrass metrics strongly correlated with traditional metrics, but linear regressions of epiphyte biomass vs. epiphyte area (pixels) and biomass ratio of epiphyte to seagrass vs. epiphyte coverage (epiphyte pixels/leaf pixels) were weaker. This was likely due to seasonal and environmental influences on both the epiphyte community composition and the seagrass-epiphyte relationship, since image analysis does not capture the depth of epiphyte growth on the leaf. The image analysis method provides insight into the spatiotemporal accumulation of epiphytes on the seagrass host and has the potential to be adapted to detect environmentally-induced changes in the community composition of epibiota.

Key word: Epiphyte, Image analysis, Seagrass, Seagrass-epiphyte relationship; Algae; Biofilm; Environmental conditions, Biomass ratio; Leaf coverage; Community composition

1. Introduction

Seagrasses are important marine plants that provide multiple ecological services to coastal ecosystems (Hemminga and Duarte, 2000). Seagrass beds enhance biodiversity and provide habitat for marine organisms in different life stages, including commercially important species (Duffy, 2006; Heck et al, 2003). As major primary producers, seagrasses supply organic carbon and food resources for marine organisms inhabiting tropical and temperate areas (Heck et al., 1997; Orth et al., 2006; Van Katwijk et al., 2016). Seagrass systems also play significant roles in filtering nutrients flowing into coastal ecosystems and stabilizing sediments to store blue carbon derived from leaves and rhizomes (Greiner et al., 2013). As major components in seagrass ecosystems, epiphytes contribute high productivity, sometimes exceeding the biomass of the seagrass host (Orth and Van Montfrans, 1984). Observation of invertebrate feeding behavior and isotope tracking indicated that epiphytic algae can be the primary food resource in seagrass meadows (Kitting et al., 1984; Nielsen and Lethbridge, 1989). Primary production in Mississippi Sound included seagrass, epiphytic algae, sand microflora and phytoplankton, with the dominant producer being epiphyte algae (Moncreiff et al. 1992). However, excessive accumulation of epiphytes can be detrimental

to seagrass, or even the whole coastal ecosystem (Bulthuis and Woelkerling, 1983). It has been suggested that seagrass plant morphology is affected as a response to competition with epiphytes for light and nutrients (Frankovich and Fourqurean, 1997; Ralph et al., 2007; Ow et al., 2020). Light attenuation is the major limiting determinant of seagrass presence by decreasing its photosynthesis (Dennison and Alberte, 1985, 1986; Ralph et al., 2007; Nelson, 2017a). Due to eutrophication, fast-growing epiphytes may reduce the light penetration to the leaf by intercepting the light to reduce productivity. Conditions of eutrophication-induced phytoplankton blooms, turbidity from sediment disturbance, and/or overgrowth of epiphytes reduce light availability. Light below a variable threshold of 4-36% surface irradiance limited seagrass photosynthesis (Dennison et al., 1993). Ammonia uptake by seagrass leaves was also reduced with increasing epiphyte coverage (Cornelisen and Thomas, 2004) and there may be effects on carbon uptake and oxygen supply (Sand-Jensen, 1977; Brodersen et al., 2015). These mechanisms may explain in part why excessive epiphyte growth is considered one of the factors contributing to seagrass decline. Thus, Nelson (2017b) developed a quantitative method to establish a threshold of epiphyte load as an indicator of eutrophication in coastal ecosystems. Epiphyte loading, controlled by both bottom-up and top-down processes

(Heck and Valentine, 2006, 2007; Peterson et al., 2007; Whalen et al., 2013), is thus an integrated indicator of environmental influences.

Because of the ecological importance of seagrass, scientists have monitored epiphyte accumulation on seagrass blades to evaluate impacts on seagrass health (Borowitzka et al., 2007; Burkholder et al., 2007; Whalen et al., 2013). The seagrasses are not just simple substrata for epiphytes, rather, the epiphytes may select suitable seagrass leaves because of positive or negative interactions (Pinckney and Micheli, 1998). Recent works about diverse microbe-seagrass mutualism and the defense systems of the seagrass against the epiphytic microorganisms indicated complex biochemical interactions between epiphytes and their seagrass hosts (Crump et al., 2018; Papazian et al., 2019). The interaction between seagrass hosts and their associated epiphytic algae communities could change dramatically due to variable environmental factors, including light, water temperature, nutrient levels, and grazing effects (Nelson and Waaland, 1997; Armitage et al., 2006; Heck and Valentine, 2006; Whalen et al., 2013; Mabrouk et al. 2014). Hence, understanding the patterns of epiphyte accumulation on seagrass blades could provide important

insight into changes in the epiphyte-seagrass dynamics and associated environmental conditions.

Understanding seagrass responses to environmental change requires consideration of physiological, morphological, and community consequences. This requires accurate assessment of morphological changes as an immediate temporal response (McMahon et al., 2013). Biomass, leaf length and width, and seagrass bed distribution and areal coverage are common indicators used for seagrass condition assessments in large scale monitoring projects (Neckles et al., 2012; McMahon et al., 2013; Congdon and Dunton, 2016; Hobson and Whisenant, 2018). Epiphyte accumulation is also an indicator of environmental conditions (McMahon et al., 2013; Nelson, 2017b) and the dominant methods focus on biomass, including dry weight biomass and ash-free dry weight biomass (Dry organic weight) (Heijs, 1984; Peterson et al., 2007). Alternative measures utilizing pigment quantification or visual microscopic examination also identified patterns of epiphyte accumulation on seagrass (Armitage et al., 2006; Corlett and Jones, 2007; Ow et al., 2020). The epiphyte composition was distinguished by relative concentrations of photopigments including chlorophyll *a*, chlorophyll *b*, fucoxanthin, and zeaxanthin (Pinckney and Micheli, 1998;

Armitage et al., 2006) which represented the biomass of different microalgal groups.

Epiphytes on seagrass are typically collected by scraping gently from host plants. Some studies removed epiphytes from rooted macrophytes by shaking in bottles with low pH MES buffer (Zimba and Hopson, 1997), or preprocessing with dilute acid for removing calcareous epiphytes (Bulthuis and Woelkerling, 1983; Alcoverro et al., 1997). Other mechanical methods used water flow (Hickman, 1971), or scraping after lyophilizing on dry ice (Penhale, 1977). The traditional epiphyte removal and biomass measures are simple and inexpensive to perform, but they are somewhat tedious and may fail to account for community species composition or morphology changes at the seagrass leaf level, and thus provide limited and incomplete spatiotemporal information regarding response to a changing environment. Other alternative evaluations, such as photopigment quantification demonstrate the variability of epiphyte coverage and community assemblages, but they do not easily reveal the spatial and temporal patterns of epiphyte accumulation on seagrass leaves that could be important for understanding how the seagrass-epiphyte dynamic relationship changes in response to environmental factors. It would be helpful to develop other easily accessible technologies to obtain greater

spatiotemporal resolution in assessment of epiphyte coverage, accumulation, and epiphyte community composition changes.

The objective of this study was to develop a robust image analysis technique for monitoring the spatiotemporal epiphyte accumulation on *Thalassia testudinum* leaves, and to provide some validation of the method and its utility. *T. testudinum*, the subject of this study, is a climax species and one of the three most prevalent seagrass species in the Gulf of Mexico (with *Syringodium filiforme* and *Halodule wrightii*) (Dunton et al., 2010; Congdon and Dunton, 2016). The relatively long-lived *T. testudinum* leaves provide surfaces to which microorganisms, algae, and invertebrates readily attach and grow (Corlett and Jones, 2007; Michael et al., 2008). With the development of advanced digital photography and computer science, the widespread application of image-analysis in many plant studies makes these methodologies particularly attractive for seagrass and epiphyte analyses (Boese et al., 2008; Shamir et al., 2010; Golzarian et al., 2011; Campbell and Fourqurean, 2014; Canonico et al., 2019). For example, Boese et al. (2008) used ERDAS ER Mapper software, which is widely applied in geospatial image analysis, to analyze injury on seagrass leaves. More recently, image analysis was used to surveil for eelgrass wasting disease on scanned leaves (Aoki et al., 2022), and

for assessment of epiphyte coverage on scanned leaves (Mehrubeoglu et al., 2021; Huang et al., 2023).

In this work, a color scanning and image analysis-based method was developed to process scanned RGB color images of seagrass blades to distinguish epiphyte-colonized vs. uncolonized leaf areas of *T. testudunum*. High-resolution pixel classification was derived from the spectral information and validated to accurately quantify the seagrass leaf area morphology, as well as the pixel areas corresponding to diverse epiphytes collectively vs uncolonized seagrass. The image-derived proportion of leaf area colonized by epiphytes (Leaf Coverage) is inferred to represent the growth rates of seagrass leaves and colonizing epiphytes relative to each other, providing unique insight into the epiphyte-seagrass relationship that is compared to the epiphyte/seagrass biomass ratio (epiphyte load). This work presents the development and validation of the image analysis method using the same experimental samples that were previously analyzed in relation to seasonal and environmental nutrient variation (Huang et al. 2023).

2. Method

2.1 Seagrass collection and processing

Shoots of *Thalassia testudinum* were collected from persistent turtle grass beds (27°52'55"N; 97°08'55"W) adjacent to the Intracoastal Waterway (ICWW) and near Redfish Bay located on the northwestern Gulf of Mexico (Figure 1A). Two study areas (Figure 1B) on the north and south sides of a man-made peninsula with an RV Park were chosen because of their proximity, different exposure to anthropogenic nutrients and visual distinctions between epiphytic communities. The north area is near a wastewater treatment plant (WWTP) effluent discharge site, and the south area (Control) is farther away from a second wastewater treatment plant effluent release site that also includes mitigating nutrient filtration through a wetland system. Within the Control and WWTP areas, there were 3 sampling sites that differed by depth (Table 1), labeled Shallow (S), Medium (M) and Deep (D). The Control M site was replaced by a special site (CI) in the south area that was close to the ICWW and adjacent to a shallow oyster reef. CI had the highest dissolved inorganic nitrogen (DIN) and the highest epiphyte loading compared to Control and WWTP areas (Huang et al. 2023). From July 2019 to April 2020, *Thalassia. testudinum* was collected monthly or bi-monthly. The volume and time requirements of sample processing work necessitated staggered visits to the south and north sampling areas at approximately three-week intervals.

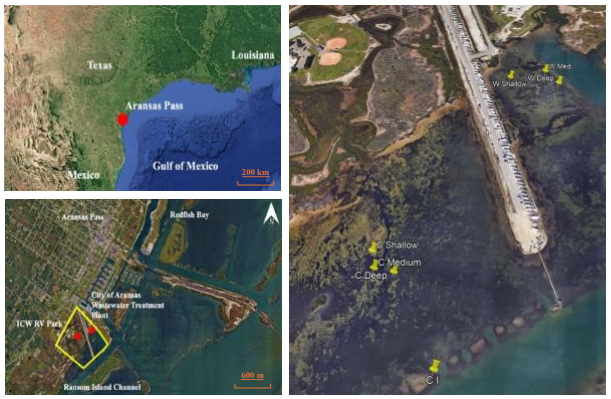

Figure 1. (A) Map of the Texas Coastal Bend and (B) the Aransas Pass-Redfish Bay sampling area (Yellow boundary area). The maps are from Google Earth. Red dots represent two permitted WWTP discharge sites. (C) Enlargement of the yellow boundary area in A. Unmanned Aerial Vehicle (UAV) imagery of study area courtesy of Dr. Hua Zhang at TX A&M University-Corpus Christi. The "Control" site is south of the RV park, comprising shallow (CS) and deep sites (CD). The "WWTP" area is north of the RV park, comprising shallow (WS), medium (WM) and deep (WD) sites. The Control ICWW (CI) site showing the highest epiphyte loading is also located.

Table 1. Depth and GPS coordinates for 6 sampling sites in Aransas-Redfish Bay Study area, Texas

Sampling Location	Mean Depth (cm)	Standard Deviation	Minimum Depth (cm)	Maximum Depth (cm)	GPS Coordinates
Control Shallow (CS)	58.0	13.0	45.0	88.0	W 027.88053 N 097.15044
Control Deep (CD)	83.3	13.4	65	107	W 027.88021 N 097.15002
Control ICWW (CI)	47.2	11.9	35	73	W 027.88053 N 097.15044
WWTP Shallow (WS)	67.2	17.8	29	95	W 027.88485 N 097.14861
WWTP Medium (WM)	79.3	16.6	46	110	W 027.88467 N 097.14790

WWTP Deep (WD)	93.2	16.5	62	125	W 027.88435 N 097.14761

For each sampling, all seagrass shoots were harvested within three haphazardly placed "rings" at each site for triplicate replication. Rings consisted of a thin slice of a 7.6 cm inner diameter PVC pipe, encompassing an area of 4.53×10^{-3} m^2. Seagrass shoots and leaves angled by the current were gently re-positioned so that every leaf, of every shoot that was located within the ring, was contained entirely within the ring. Leaves of shoots anchored outside the ring were excluded from the ring. Then all seagrass shoots anchored inside the ring were harvested by reaching down into the sediment and plucking, keeping all leaves still attached to their shoot. Representation of young shoots was obtained in this manner. This sampling strategy is important for capturing variation in the different states (ages) of seagrass growth and epiphyte accumulation. Seagrass samples were collected in plastic bottles, placed on top of ice for transport, and stored at 4-10 ℃ in the laboratory.

Initial sample processing in the laboratory was completed within 72 hours of harvest. Seagrass samples were gently soaked for 2-3 minutes in deionized water to remove salt and loose non-specifically associated material (e.g., sand). The green portion of

leaves were removed from a single whole shoot at the junction with the leaf sheath, measured for morphometrics (leaf length and width), and then arranged on a fluid mount scanning tray for the Epson Perfection V-750 Pro color flatbed scanner (Epson, Carson, CA). Leaf images were obtained using 24-bit color scanning at 1200 dpi resolution and then saved as .tiff files (Figure 2). After scanning leaves, epiphytes were removed from seagrass blades by scraping with a microscope slide into a small volume (<10 mL) of deionized water. Subsequently, the epiphytes and the epiphyte-free leaves were dried to constant weight at 60°C for biomass measurement. The leaves were not re-scanned after epiphyte removal in this study because sometimes there is damage to the leaves that compromises a second image analysis. However, preliminary studies (data not shown) showed epiphyte removal efficiency to typically be >90%.

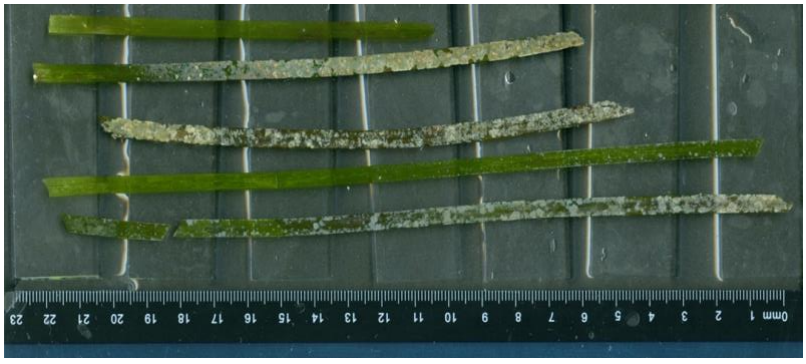

Figure 2. Scanning picture of one *Thalassia.testudinum* shoot from "Control" area (Lightened by 15%).

2.2 Image analysis

Scanned images were analyzed in the ENVI 5.0 program (L3 Harris Technologies, Ohio). This geospatial analytics software is widely used for earth science, construction, and vegetation research, including several seagrass mapping studies (Lyons et al., 2011; Canty, 2014). Here, it was applied on a micro-level to analyze epiphyte accumulation on the leaf surfaces. The area of each seagrass leaf and associated epiphytes were recorded by counting the pixels of the uncovered and covered areas of the leaf, respectively. The proportional coverage of the seagrass leaf by epiphyte was considered to be an indicator of epiphyte recruitment and growth relative to seagrass growth.

The pixels of background and other non-analyzed contents were edited to appear as mask pixels by manually creating an outline around each seagrass blade. The edited leaf images were then analyzed by Spectral Angle Mapper (SAM) classification to distinguish the uncolonized seagrass leaf and areas covered by epiphytes. As a leading classification method in various studies, the SAM algorithm is implemented in ENVI to compare image spectra directly (Yuhas et al., 1992; Kruse et al., 1993). In a true-color image, the standard creation of different colors in each pixel is produced by combining three values that represent the

reflectance from the red, green, and blue (RGB) bands. Each of these bands is digitally numbered from 0 (no reflectance) to 255 (maximum reflectance). The three bands are treated as three spectra by ENVI. By considering each pixel with three spectra as a vector, spectral information of each pixel can be transformed into a vector in a three-dimensional cartesian coordinate system (R, G, B). The SAM algorithm quantifies the similarity (difference) between the pixel spectrum and the reference spectrum by the magnitude of a spectral angle (Kruse et al., 1993).

Classifications of seagrass leaf vs epiphytic coverage were estimated by evaluating the degrees of the spectral angles between the pre-established reference spectra and the test spectra. The reference spectra were selected by the minimum, mean ($\pm$SD), and maximum of spectra in multiple manually captured areas (1000~5000 pixels), which were visually classified as seagrass or epiphytes, from approximately 200 scanned images. The seagrass leaf images for building seagrass and epiphyte reference spectra were from the samples harvested in the “Control” and “WWTP” areas in August 2019. A random seagrass blade image was pre-analyzed to further select the applicable reference spectra. Through visual inspection, reference spectra that misidentified seagrass and epiphyte pixels were eliminated from the spectral reference

libraries. Remaining spectra were combined, respectively, to produce a seagrass spectral library and an epiphyte spectral library. The seagrass spectral library contained 482 reference spectra, which included the uncolonized area of seagrass blades which had somewhat different colors due to variable age, growth and health status, and possibly due to undetected presence of microbiota. The epiphyte spectral library contained 843 reference spectra from a mixed group of diverse epiphytic components. 2,061 edited leaf images (background removed) were analyzed using both the seagrass and epiphyte spectral libraries. The threshold of spectral angle identification was set on 0.04 angle radians (≈2.3°) based on visual estimation from pre-analysis. The pixels were identified as seagrass, epiphytes, or unclassified content by calculating their spectra's similarity (or lack thereof) to the corresponding reference spectra through the ENVI program.

2.3 Output Validation

After classifying the images, two types of validation methods, referred to as “Intrinsic Validation” and “Extrinsic Validation”, were used to calculate the accuracy of identified seagrass and epiphyte pixels. Pixels identified from seagrass and epiphyte spectral libraries were compared with each other and to ground-truth pixels as “Intrinsic Validation” of the proportion of correctly

identified pixels. From another approach, the process of "Extrinsic Validation" compared the imaging-derived metrics with traditional biomass metrics to observe the correlation between the two types of indicators. The image-based measurement is considered to be valid if the error from "Intrinsic Validation" is sufficiently small (<10%), and if there is a goodness of fit between the image classification outputs and biomass measurements in "Extrinsic Validation".

2.3.1 "Intrinsic Validation"

Ideally, all pixels should be uniquely classified by one of the two spectral libraries as bare seagrass leaf or epiphyte. The percent cover of epiphytes on each leaf was calculated from the seagrass (*SG*)- and epiphyte (*Epi*)-classified images (Figures 3B and 3C) and compared. This validation procedure quantified the discrepancy (the difference between epiphyte coverage estimated from the seagrass and epiphyte spectral libraries). The discrepancy corresponded to the percent of the area in the classified images that was incorrectly classified. The percent cover by epiphyte in *SG*- and *Epi*-classified images was calculated as follows:

$$\text{Percent Cover of Epiphyte } (SG) = \text{(pixels of unclassified area) / (pixels of total leaf area)} \times 100\%$$

(Eq. 1)

Percent Cover of Epiphyte (*Epi*) =

(pixels of identified epiphytes) / (pixels of total leaf area)×100%

(Eq. 2)

where, the pixels which could not be identified as seagrass by the seagrass spectral library, listed as "pixels of unclassified area" in Eq. 1, were ideally counted as epiphytes.

The number of unclassified pixels, identified epiphyte pixels, and total leaf area pixels were tallied by the ENVI program. The identification of epiphytes and seagrass was considered to be valid if the absolute difference in percent cover of epiphytes between *SG*- and *Epi*- images had a small value (<10%), which suggested that the unclassified area in *SG*-classified images matched the epiphyte area identified in the *Epi*-classified images.

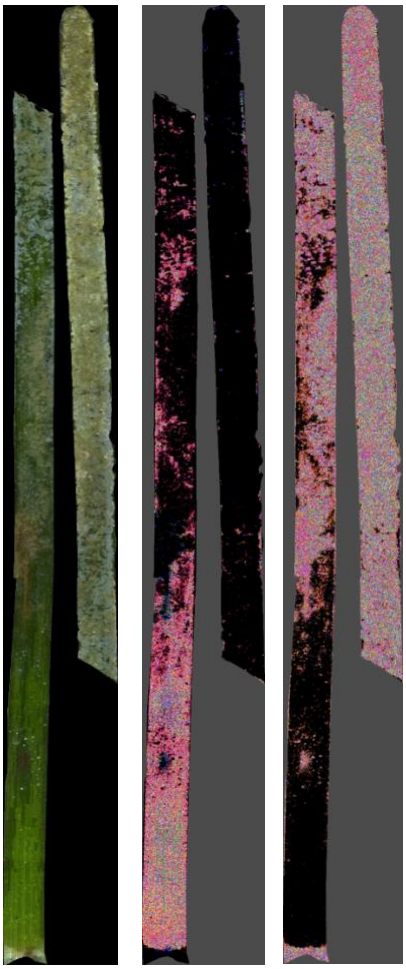

A B C

Figure 3. An example of seagrass blade color scans (A) and ENVI classification of seagrass and epiphyte (B and C respectively) collected from Control area on July 31, 2019. The black areas are the unclassified pixels using a particular spectral library (NOT seagrass in (B), and NOT epiphyte in (C)). (A) original scanned blade; (B) seagrass classified Image (ENVI); (C) epiphyte classified image (ENVI). Images lightened by 15%.

The classification outputs were also evaluated by "overlap analysis", which quantified misclassified pixels by "overlapping" the *Epi* images entirely over the corresponding *SG* images. The

output of overlap validation created three kinds of pixels, including correctly paired pixels, “overlapping” pixels, and “unaccounted” pixels. The paired pixels were those that were uniquely identified by either the seagrass or the epiphyte spectral libraries. If the pixels were identified as both seagrass and epiphytes by the two spectral libraries simultaneously, they were regarded as “overlapping” pixels. Pixels that could not be identified by either seagrass or epiphyte libraries were regarded as “unaccounted” pixels. This overlap analysis thus reveals the proportion of indeterminate pixels, those not uniquely identified, and is important in the validation of the method.

To decrease bias from variance between sites and seasons, images of three seagrass shoots from each sampling time at each site were selected randomly for overlap analysis. Four hundred and seventy-nine *SG*-classified leaf images were compared with corresponding *Epi*-classified images by overlapping with each other. The selected images were converted to grayscale in MATLAB 2019b (Mathworks, Inc) as a weighted sum of R, G, B spectral values. Pixels were represented as grayscale with a single value spanning from 0 to 255. Afterwards, the classified pixels were set to a mid-gray value (120). The manually determined background value was converted to 255 (white) and then excluded from the analyses. The

values of ENVI-based non-classified pixels in both *SG*- and *Epi*-classified images were kept at 0 (black) as original, and the ENVI-based identified pixels, which either identified as seagrass or as epiphytes, were all converted to a single middle value "A" between 0 and 255 (Figure 4). This single value "A" was selected arbitrarily to be less than 127 in each image for overlap analysis. The overlapping and unaccounted pixels were located by adding the converted *SG*- and *Epi*-classified images. The grey value of paired pixels would stay at the value "A". However, the overlapping and unaccounted pixels would produce a double "A" value and zero value, respectively (Figure 5). The number of overlapping pixels, unaccounted pixels, and total leaf area pixels were tallied using MATLAB 2019b. The number of indeterminate pixels was calculated as the sum of overlapping seagrass or epiphyte pixels and overall unaccounted pixels (pixels that were unaccounted both from seagrass spectral library and epiphyte spectral library results' analysis).

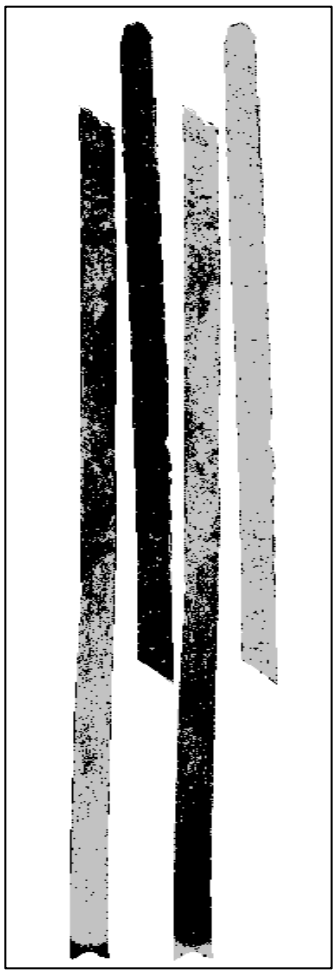

A B

Figure 4. "A" value converted images from Figures 3B and 3C. (A) epiphyte segmentation (black), background (white), and epiphyte-free seagrass blade area (single gray); (B) epiphyte-free seagrass blade area (black), background (white), and epiphyte segmentation (single gray). Images lightened by 15%

A B

Figure 5. Overlapped image from Figure 4A and 4B. (A) The epiphyte segmentation (black) from Figure 4A and the epiphyte-free seagrass blade area (black) from Figure 4B are complementary in the overlapped image. (B) Enlargement of the red box in A. The background (dark red), unique pixels (blue), and overlapping pixels (cyan) are shown. Color is adjusted to enhance distinction.

2.3.2 "Extrinsic Validation"

In the "Extrinsic Validation" of seagrass metrics, total seagrass leaf pixels were correlated to dry weight leaf biomass and morphometrics measures (e.g., leaf length or leaf area). For

"Extrinsic Validation" of epiphyte imaging metrics, epiphyte-classified pixels of each leaf were correlated to epiphyte dry weight biomass of each leaf, and for relative comparisons, the percent leaf coverage ((epiphyte pixels/total leaf pixels) x 100) was correlated to biomass-based epiphyte loads (Epiphyte biomass/leaf biomass) (Fong and Harwell, 1994). Scatter plots of traditional biomass and morphology metrics vs. image-based metrics for seagrass (n = 2052) and epiphyte (n = 1822) measures were created to evaluate their correlations.

2.4 Statistical Analysis

The outcomes from the "Intrinsic Validation" in the "Control" area, "WWTP" area, and CI site across six sampling times were evaluated to investigate spatiotemporal effects of epiphyte colonization on the image analysis. The different sampling times in the "WWTP" area, "Control" area, and CI site precluded a simultaneous location-comparison of "Intrinsic Validation" outcomes. Therefore, data were reallocated to four seasons based on the sampling date and average water temperature (Huang et al. 2023) to facilitate comparisons by location. A one-way analysis of variance (ANOVA) was performed to evaluate the significant differences ($P < 0.05$) for the absolute difference in epiphyte coverage between *SG*- and *Epi*-classified outputs via *R* program.

Linear regression analyses were used to evaluate the "Extrinsic Validation" of the seagrass and the epiphyte imaging metrics. Manually measured leaf length and area, and epiphyte-free leaf biomass were tested for linear correlation with image-derived seagrass leaf area (i.e., total leaf pixels). The linear regression between epiphyte biomass per seagrass leaf and image-derived epiphyte covered area (i.e., identified epiphyte pixels) was also analyzed. The epiphyte load (epiphyte biomass/seagrass biomass) (Fong and Harwell, 1994) and the image-derived percent cover of leaf by epiphytes (epiphyte coverage; see Eq.2) were analyzed by linear regression to quantitatively assess accuracy of imaging metrics. The linear regression analyses used R Studio and were assessed by R^2 values.

3. Results

3.1 Example Seagrass Leaf Scans

A true color image of a segment of epiphyte-covered *T.*. *testudinum* leaf and the classification outputs of seagrass and epiphytes obtained from the image classification procedure are shown in Figure 3. A seagrass-classified image (Figure 3B) presents variable uncovered seagrass leaf details, such as growing

areas (appearing as different green levels) and damaged or senescing areas (appearing as different yellow or brown levels), with 482 uncovered leaf classes. The black area on the seagrass-classified example is the unclassified area, ideally representing the epiphyte covered area. Epiphyte covered regions classified by epiphyte spectral reference libraries (Figure 3C) presented 843 classes, with the black areas representing uncovered seagrass leaf distinguished by the ENVI program. Multiple image classes may represent the same feature (e.g., uncovered leaf or an epiphyte species) if there were visual differences on different leaves or areas on the same leaf.

Within the 843 epiphyte reference spectra, four dominant color groups were usually observed on the images of *T. testudinum* leaves in the study area, including a reddish-white group, a red group, a yellowish-brown group, and a green group. The reddish-white group comprises white and pink pixels, which primarily contains small *Serpulid* worms, coralline red algae, and several unidentified species (Figure 6A). The red group combines pixels of several filamentous red algae or bryozoans (Figures 6B and 6C). The yellowish-brown group includes pixels which can be recognized as yellowish or brownish filamentous *Chlorophyta* groups, as well as the yellowish tint of old chlorotic seagrass

leaves (Figure 6D). A small number of unidentified species are recognized in this group as well. Lastly, the green group contains RGB features of multiple green levels, which may identify as young uncolonized seagrass blades or epiphytic green algae (Figure 6E).

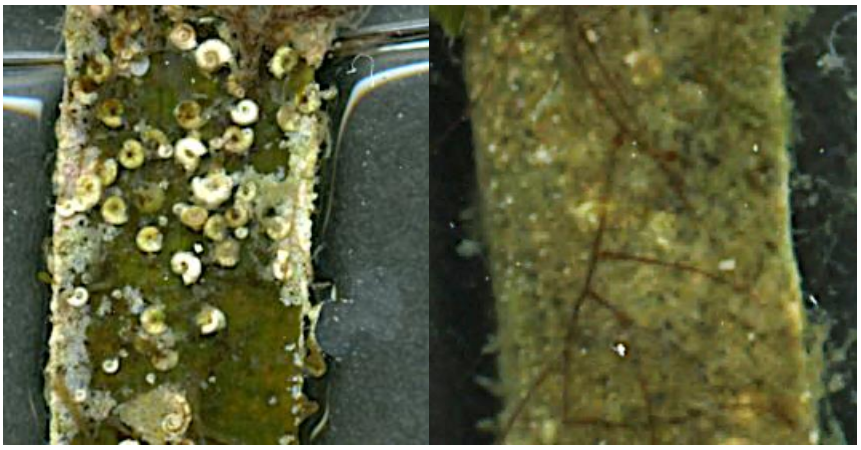

A B

C D

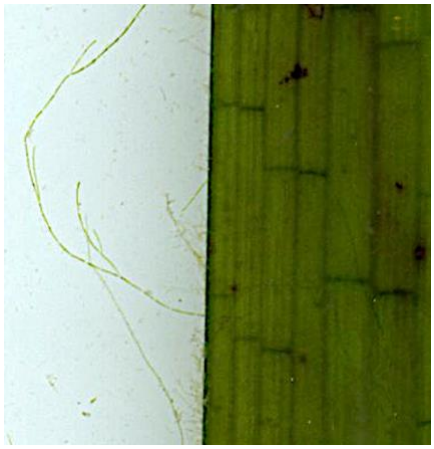

E

Figure 6. Four major color groups are distinguished by seagrass leaf image analysis: (A) *Serpulid* worms (center) *vs.* coralline red algae (edge, pink is living algae, and the white is dead) present on a seagrass blade (enhanced by 100% sharpness). (B) Filamentous red algae present on a coralline algae layer (enhanced by 50% sharpness and 30% brightness). (C) Epiphytic bryozoan can be mis-identified as filamentous algae (enhanced by 100% sharpness). (D) Clumps of yellowish green algae over dead coralline algae on a senescent brownish-green seagrass blade (enhanced by 100% sharpness and 40% brightness). (E) Filamentous green algae present on the edge of a bright green seagrass blade (enhanced by 100% sharpness and 40% brightness).

3.2 "Intrinsic Validation": Comparison of Percent Epiphyte Cover of Leaves

"Intrinsic Validation" assessed how effectively all of the pixels of the leaf images were classified. Epiphyte coverage of the seagrass leaf was evaluated by counting pixels identified as seagrass leaf or epiphyte through the respective spectral libraries. Areas identified as epiphytes on the *Epi*-classified images should correspond to

areas not characterized as seagrass leaf on the *SG*-classified images. Analysis of 2,001 scanned images of seagrass blades found that the absolute value of the difference in epiphyte coverage between *SG*- and *Epi*- classified images (see Eq. 1 and Eq. 2, Methods) was < 10% in 94.45% of the classified output. 83.01% of the outputs showed < 5% absolute difference.

The absolute difference in epiphyte coverage showed a seasonal pattern. Data for the "WWTP" area, "Control" area, and CI site were reallocated to four seasons based on the sampling date and average temperature (Huang et al. 2023) to facilitate the seasonal comparisons among locations. The average absolute difference was relatively low and consistent in summer and autumn months, but increased during late winter, and peaked during spring months. There was no significance ($P > 0.05$) to the absolute differences that appeared among the three locations from July 31 ("Control" area & CI Sites) to October 9 ("WWTP" area), which ranged from 1.91% (±1.92%) to 3.05% (±3.07%). However, the absolute difference increased strikingly and significantly from December through April in the "WWTP" area ($df = 5$, $F = 58.27$, $P < 0.05$), while the "Control" area ($df = 5$, $F = 10.59$, $P < 0.05$) and CI site ($df = 5$, $F = 24.62$, $P < 0.05$) only showed significantly higher absolute differences in April compared to other months (Figure 7).

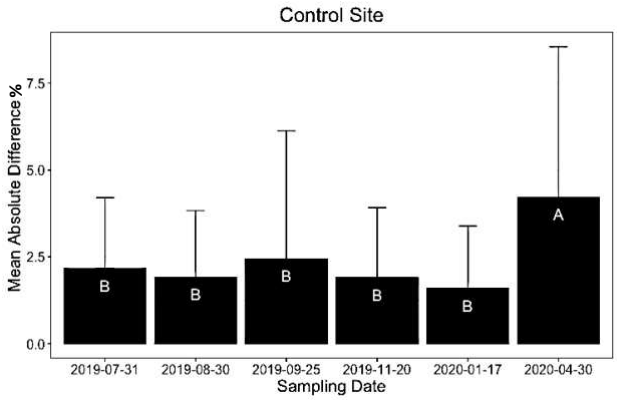

A

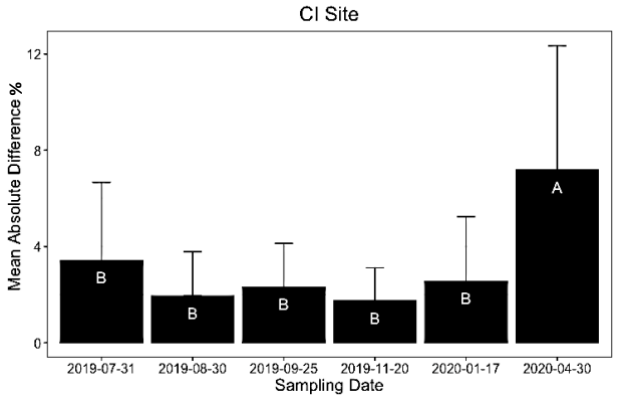

B

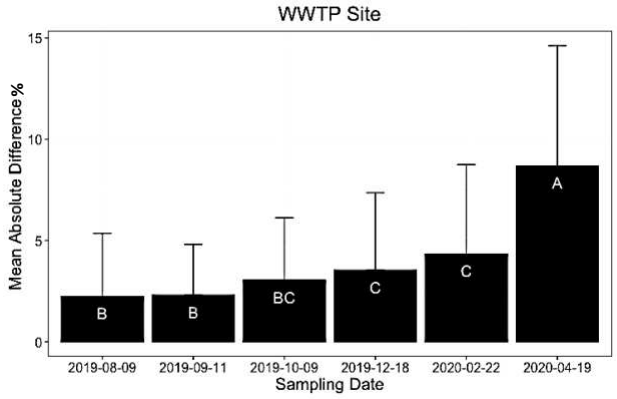

C

Figure 7. Comparison of means of absolute difference in percent epiphyte coverage (discrepancy) between *SG*-classified images (unclassified areas) and *Epi*-classified

images (classified epiphyte areas) for sampling locations of (A) "Control" area, (B) CI site, and (C) "WWTP" area, respectively. Error bars represent standard deviation, and different letters denote significant differences among 6 sampling months ($P < 0.05$).

Despite a range of discrepancy (approaching as much as 15%), between epiphyte and seagrass classifications for individual images across seasons, these absolute difference values showed a similar seasonal pattern among three sampling areas. More than 50% of analyzed images from three sampling locations in the spring had > 5% absolute difference in epiphyte coverage, whereas only 12.5% of the classified images from the other three sampling seasons had > 5% absolute difference (Figure 8A). Across the 6 sampling times, about 87.19% of blade images produced < 5% discrepancy in the "Control" area, compared to only 76.06% and 78.48% of images for the "WWTP" area and the CI site, respectively (Figure 8B).

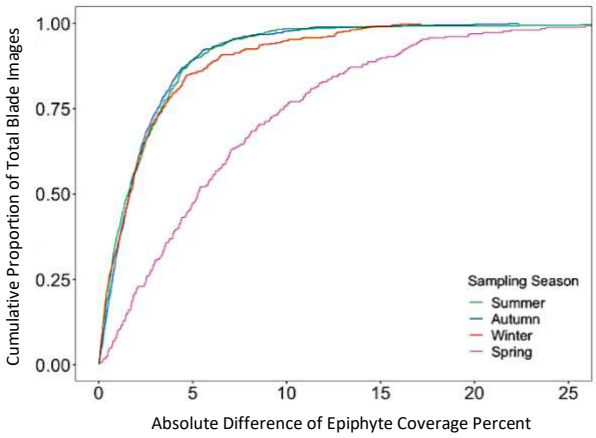

A

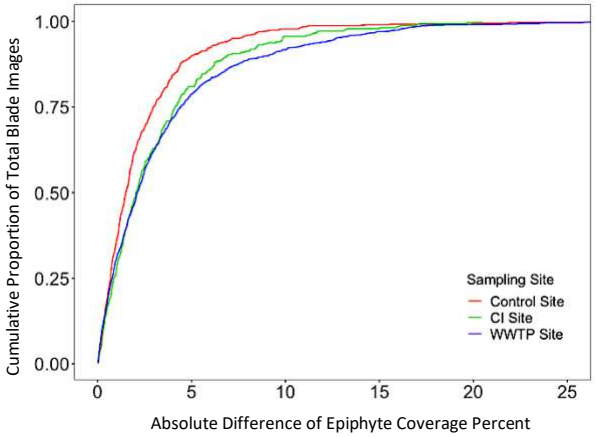

B

Figure 8. A: Cumulative distribution of absolute difference of epiphyte coverage percent between *SG*-classified images (unclassified areas) and *Epi*-classified images (classified epiphyte areas) (discrepancy) from 2019 Summer (n = 509), Autumn (n = 828), Winter (n = 452), and 2020 Spring (n = 278). Due to the non-synchronous sampling times at the three sites, data were reallocated to four seasons based on the sampling date and average water temperature to compare the magnitudes of absolute differences of epiphyte coverage by season. B: Cumulative distribution of absolute difference of epiphyte coverage at "Control" site (n = 726), CI site (n = 330), and "WWTP" site (n = 1011).

3.3 "Intrinsic Validation": Overlap Analysis

The overlap analysis was used to understand indeterminate pixels, those which could not be classified uniquely, as a combination of overlapping pixels plus unaccounted pixels. The analysis created three kinds of pixels: correctly paired pixels (uniquely identified), overlapping pixels (misclassified in *SG*- or the *Epi*-classified images), and unaccounted pixels (not identified in either classification).

The overlap analysis reported unique seagrass and epiphyte pixel identification > 90 % in 94.57% of the analyzed images (Figure 9). The percent of indeterminate pixels varied from 0.21% to 31.50%, with a mean value of 4.47% (Table 3). About 90% of the images had < 10% indeterminate pixels. Overlapping pixels accounted for 1.98% on average (Table 3; Figure 9). The amount of the unaccounted pixels, which were not identified by either seagrass libraries or epiphyte libraries, averaged 2.48% (Table 3).

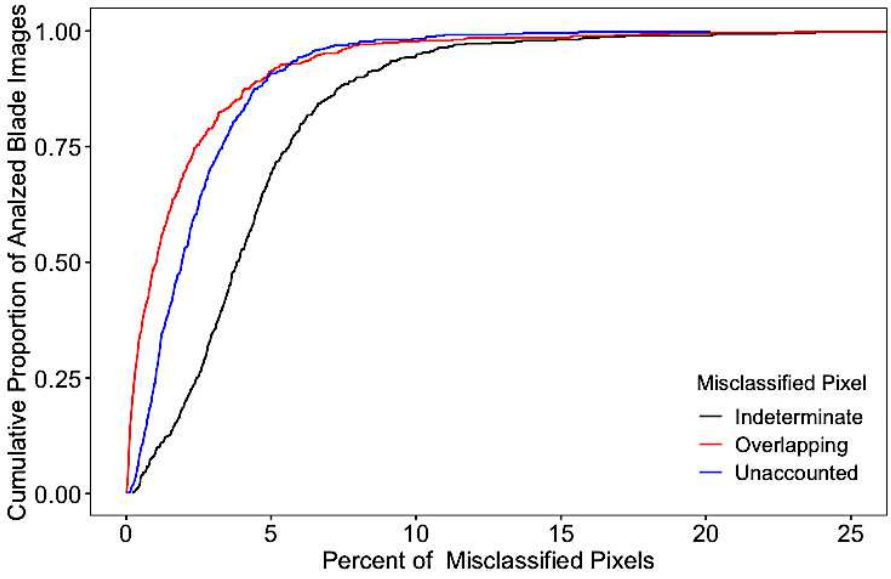

Figure 9. Cumulative distribution of indeterminate pixels (black), overlapping pixels (red), and unaccounted pixels (blue) of the 479 random images for overlap analysis.

Table 3. Minimum, maximum, and average percent (±SD) of the indeterminate, overlapping, and unaccounted pixels in the images for overlap analysis.

Pixel Types	Minimum Percent of Pixels	Maximum Percent of Pixels	Average Percent of Pixels
Indeterminate Pixel	0.21%	31.50%	4.47% (±3.41%)
Overlapping Pixel	0.01%	31.50%	1.98% (±3.04%)
Unaccounted Pixel	0.00%	20.12%	2.48% (±2.24%)

3.4 "Extrinsic Validation": Comparative metrics for seagrass

The "Extrinsic Validation" evaluated the correlation between the imaging and the traditional biomass and morphometric assessments of seagrass and epiphytes. The comparisons for seagrass showed strong linear relationships between the manually measured seagrass leaf area and the imaged seagrass leaf area (R^2 =

0.98, P < 0.0001, n = 2052; Figure 10A) and between leaf length and imaged leaf area (R^2 = 0.86, P < 0.0001, n = 2053; Figure 10B). The relationship between dried leaf biomass and imaged leaf area was also strong (R^2 = 0.88, P < 0.0001, n = 2048; Figure 10C). These strong correlations support utility of imaging for seagrass monitoring.

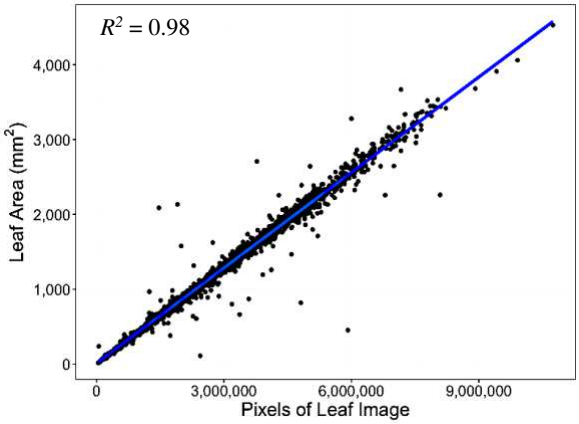

A

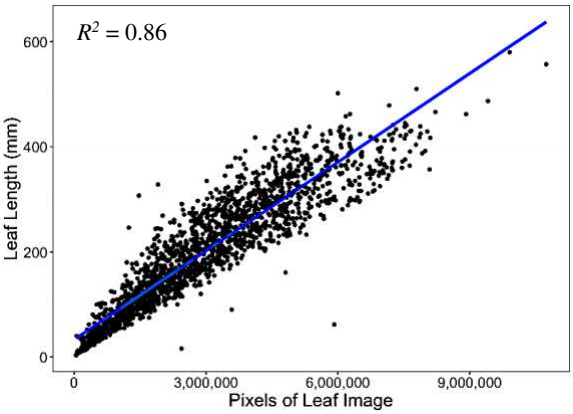

B

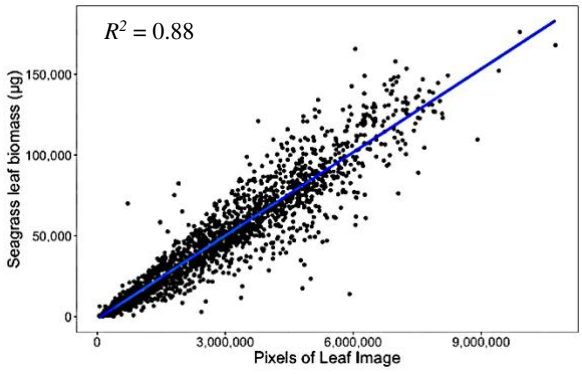

C

Figure 10. The relationships between manually measured seagrass leaf morphometrics and the number of leaf-image pixels: A) the manually measured leaf area and leaf-image pixels, the best fit regression: Manually measured leaf area = 0.42 × 10^{-3} Total number of image pixels + 11.8 (R^2 = 0.98, P < 0.0001, n = 2052); B) the manually measured length of seagrass leaf and leaf-image pixels, the best fit regression: Leaf length = 5.63 ×10^{-3} Total number of image pixels + 33.21 (R^2 = 0.86, P < 0.0001, n = 2053); and C) leaf biomass and leaf-image pixels, the best fit regression: Leaf biomass = 17.20 × 10^{-3} Total number of image pixels – 1449 (R^2 = 0.88, P < 0.0001, n = 2048).

3.5 "Extrinsic validation": Comparative metrics for epiphyte accumulation

The linear correlation of epiphyte biomass to the total number of identified epiphyte pixels (Figure 11A) was moderate (R^2 = 0.61, P < 0.0001, n = 1915). Epiphyte accumulations on seagrass leaves are often considered from a relative perspective. Epiphyte metrics may be normalized to seagrass host metrics, such as leaf biomass or leaf area. Figure 11B compared normalized epiphyte accumulation metrics from imaging and biomass. Epiphyte load (epiphyte biomass/seagrass biomass) was linearly correlated

735 with % epiphyte coverage moderately but significantly (R^2 = 0.52,
736 P < 0.01, n = 1817; Figure 11A). There two models both showed
737 linearity, homoscedasticity, and normal distribution.

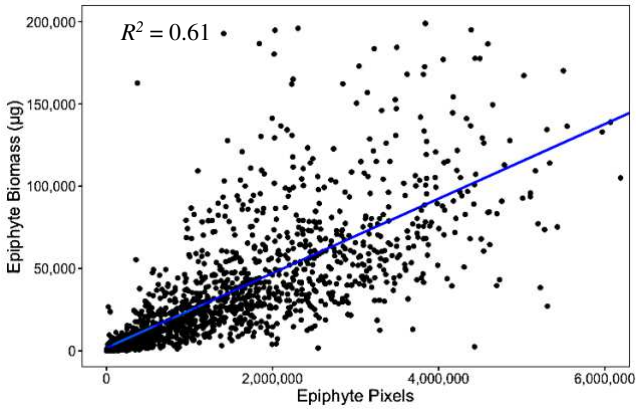

738 A

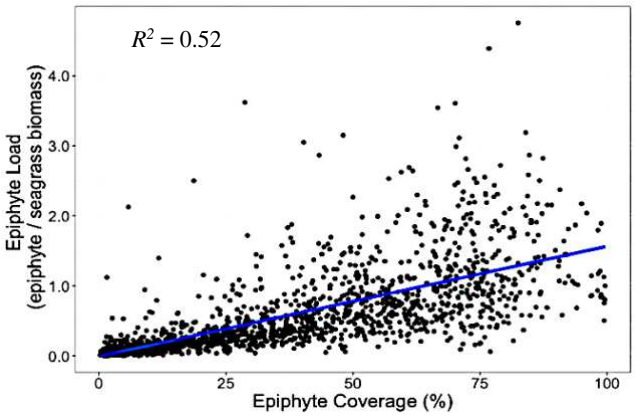

739 B

740 **Figure 11. A: The best fit linear regression between epiphyte biomass per leaf (µg)**
741 **and the epiphyte covered area based on the number of identified epiphyte pixels for**
742 **the three sampling areas over the six sampling times. The best regression equation:**
743 **Epiphyte biomass = 15.70 × 10^{-3} Epiphyte pixels + 1902 (R^2 = 0.61, P < 0.05, n =**
744 **1815). B: The relationship between epiphyte load (epiphyte dry weight/seagrass dry**
745 **weight) and epiphyte coverage (%) classified by the epiphyte spectral library.**
746 **Epiphyte load is calculated by dividing the epiphyte dry biomass by seagrass leaf**
747 **biomass. The best regression equation: Epiphyte load = 15.70 × 10^{-3} Epiphyte**
748 **coverage (%) – 0.07 (R^2 = 0.52, P < 0.0001, n = 1817).**

749

4. Discussion

This study developed an efficient and informative method to scan seagrass leaves using accessible, inexpensive color scanning technology. The image analysis performed here utilized a commercially available program (ENVI, NV5 Geospatial Solution, US) with a menu-driven mode, and many image-processing algorithms, workflows and tutorials. It is both full-featured and accessible to persons new to image analysis. Moreover, workflows developed in ENVI can be readily adapted to open-source image analysis platforms like ImageJ (Schneider et al., 2012) or Fiji (Schindelin et al., 2012). Compared with the traditional measurements, the image-based approach offers some advantages, including ease of use, flexibility in data analysis including application of artificial intelligence (Mehrubeoglu et al., 2021; Aoki et al., 2022), image archiving for subsequent analysis or re-analysis in long-term comparisons, and ability to readily characterize epiphyte accumulation along the age gradient of each seagrass leaf.

Image analysis of scanned seagrass leaves could quantitatively distinguish the uncovered leaf areas from those colonized by diverse epiphyte taxa based on different RGB properties of

773 seagrass and epiphyte images. The utility of this method is that it
774 can generate proxy metrics for seagrass (leaf area, length, and
775 biomass), and for epiphyte accumulations (biomass). The image
776 analysis presented here effectively distinguished four major color
777 groups on a seagrass blade image. Several intrinsic and extrinsic
778 validation analyses indicate that image-based metrics for seagrass
779 growth and morphology were well-correlated with traditional
780 biomass or manual measures of seagrass shoot morphometrics.
781 However, evaluation of the image analysis method shows that
782 classification discrepancies exist. Apparent limitations of this
783 method include a less robust relationship between epiphyte pixels
784 and epiphyte biomass, compared to the relationship between
785 seagrass biomass and seagrass pixels. The robustness of the RGB
786 color-based spectral libraries used to distinguish and identify
787 image pixels as seagrass or epiphyte is an important determinant of
788 the quantification power of the method. A highly informative
789 image analysis routine, once fully developed and adapted to open-
790 source platforms, could be largely automated to make an efficient
791 additional tool for monitoring seagrasses and their epiphytes. In
792 future work, the image analysis should be improved with expanded
793 spectral libraries, automated segmentation of leaves from the
794 background, and capturing unrecognizable information through
795 artificial intelligence approaches (Mehrubeoglu et al., 2021; Aoki

et al., 2022). The AI approaches have potential to distinguish between different classes of epiphytic taxa (e.g., green, red, brown algae, bryozoans, gastropods, etc.) to extract structures of epiphytic communities and to detect their changes with environmental conditions.

4.1 Epiphyte and seagrass classification

The distinction between four dominant color groups of epiphytes classified on the images of *T. testudinum* leaves in this study suggests that the method may be useful in detecting community composition shifts. In the reddish-white group, the serpulid worms may be *Spirorbis* spp common on the basal growing *T. testudinum* leaves found in the northwestern Gulf of Mexico (Dirnberger, 1990). As the two most common coralline red algae observed along the Coast of Texas, *Melobesia* spp and *Hydrolithon* spp were also possibly classified in this group (Minnery et al., 1985; Wynne, 2008). Both diatoms and coralline red algae were reported on the tips and edges of young seagrass leaves as “pioneers” of epiphyte accumulation, which then spread dominantly (Corlett and Jones, 2007). Although the diatom community was reported as the basal epiphytic layer and entirely covered by the coralline red algae and other epiphyte groups, the scanned images in our study did not provide sufficient spatial resolution for the image analysis method

to distinguish the microalgae community. Scans could be made with greater pixel resolution, but image file sizes become very large. The red algae species in the red group resembled the *Colaconemataceae*, *Rhodomelaceae*, and *Stylonemataceae* families, which have been recorded growing epiphytically on *T. testudinum* in Florida and the southwestern Caribbean (Diaz-Pulido and Díaz-Ruíz, 2003; Albis-Salas and Gavio, 2011). Various bryozoan species, such as *Bugula neritina*, are commonly found along the central Texas coast and potentially mistaken for filamentous red algae on the scanning images (Ahrens and Grubbs, 2012). The epiphytic green algae presenting in the green group are common on seagrass along the southern Texas coast (Morgan and Kitting, 1984). Due to similar RGB characteristics, greenish epiphytes and yellowish or brownish epiphytes may be misclassified as bright green seagrass and old seagrass leaves, respectively, in the image analysis (Figures 6D and 6E). Creation of spectral reference libraries that accurately identify and distinguish epiphytes from seagrass is critical to this method.

4.2 "Intrinsic Validation" of image analysis

"Intrinsic Validation" (epiphyte classification vs. seagrass classification) and "Extrinsic Validation" (imaging metrics vs. traditional metrics) were used to assess the classification outcomes

of this image analysis method. As one of the "Intrinsic Validation" methods, discrepancy analysis revealed a low absolute difference (< 10%) in estimated epiphyte coverage between epiphyte classification and seagrass classification in > 94% of the classification output, suggesting that the ENVI program successfully distinguished most of the pixels of uncolonized seagrass and epiphytes through seagrass- and epiphyte-trained spectral libraries, respectively. The biologically important metric of epiphyte coverage is overestimated if leaf pixels are misclassified as epiphytes by the epiphyte spectral library or if seagrass pixels are not recognized by the seagrass spectral library. Similarly, uncolonized seagrass is overestimated if epiphyte pixels are misclassified as seagrass by the seagrass spectral library or if epiphytes are not identified by the epiphyte spectral library. Multiple image classes may represent different physiological states of the same feature. The image analysis likely mis-identified some greenish filamentous *Chlorophyta* groups as uncolonized seagrass leaves. Seagrass growth declined with cooler winter temperatures and the older senescing leaves presented more yellow color and brown broken edges that may have been mis-identified as yellowish green algae or brownish algae (Figures 6D and 6E). This would explain the pronounced increase in discrepancy observed in spring samples (Figure 7).

Therefore, the dramatic decrease in classification accuracy in the spring (Figure 8A) was likely due to seasonal variation in the epiphyte community which was not well-represented in the epiphyte spectral library. Note that the classifications were based on a training image dataset obtained in the summer, so the dramatic deviation in spring for all three sampling locations suggests a potential change in the epiphyte community to one with different spectral characteristics. This finding aligns with the seasonally variable algal epiphyte communities previously observed on seagrass blades (Kendrick and Burt, 1997; Reyes and Sansón, 1997; Lavery and Vanderklift, 2002; Giovannetti et al., 2010). Kendrick and Burt (1997) showed that epiphytic *Chlorophyta* groups on leaves of *Posidonia sinuosa* only presented in winter and spring in western Australia. Building spectral libraries with representation from all seasons is expected to reduce this source of image classification error.

The effectiveness of classification also differed among sampling sites, with 87% of Control site images exhibiting < 5% discrepancy, compared to 76% and 78% at the WWTP and CI sites, respectively. Previous studies showed variation of epiphytic components in response to environmental factors such as

hydrodynamics, light attenuation, water temperature, nutrient enrichment, salinity, or grazing effects (Lavery and Vanderklift, 2002; Heck and Valentine, 2006; Frankovich et al., 2009; Aumack et al., 2011). For instance, in a high light environment, leaf reddening caused by anthocyanin in *T. testudinum* was suggested to play a role of sunscreen (Novak and Short, 2011). The mature blades of *Thalassia* spp. yellowed under low salinity (Thorhaug et al., 2006), and the red : green spectral reflectance ratio of *T. testudinum* was higher in a hypersaline environment than in a hyposaline environment (Durako and Howarth, 2017). Such changes would potentially lead to the misclassification of seagrass and epiphyte pixels if using libraries not trained with these representations. In this work, salinity varied from 26 to 37. Although there was no significant difference in the mean salinity among the sampling locations, salinity levels differed significantly across seasons, being highest in the summer (Huang et al. 2023). Moreover, our unpublished 18S rRNA sequencing observations found differences in both algal epiphyte and invertebrate communities from the “WWTP” and “Control” areas. It will be important to include images from all sampling sites and experimental conditions in the training dataset.

The overlap analysis method for “Intrinsic Validation” identified indeterminate pixels as a combination of pixels being misclassified or not identified at all. Overlapping pixels reflect that the SAM algorithm did not distinguish epiphyte and seagrass pixels with similar RGB arrays based on the current reference spectra and threshold angle. Unaccounted pixels, not identified by either reference library, may be largely attributed to incomplete removal of the background, which was done manually in this study. Underestimated epiphyte coverage can result from unaccounted pixels as well. Indeterminate pixels generally represented < 10% of image pixels for seagrass and epiphyte classification in 94% of the analyzed images. Expansion and equal sample representation of the reference spectral libraries will reduce both misclassification and unidentified pixels. Additional work with other classification techniques using feature shape, texture and edge detection may improve identification accuracy. For example, the Canny edge detector (Canny, 1986) has been applied for plant leaf identification, description of leaf shape, and leaf disease pattern (Bankar et al., 2014; Codizar and Solano, 2016; Salman et al., 2017). Deep learning has been applied to seagrass image segmentation, and has potential to decrease unaccounted pixels resulting from manual segmentation (Mehrubeoglu et al., 2021).

4.3 "Extrinsic Validation" of image analysis

Image analysis-based metrics for seagrass and epiphytes were compared through linear correlations to common morphology and biomass metrics to validate the application of image analysis for seagrass investigation. Strong and significant linear relationships were found between total seagrass leaf pixels and seagrass leaf morphology (e.g., leaf area $R^2 = 0.98$, leaf length $R^2 = 0.86$) and biomass metrics ($R^2 = 0.88$). This result indicates that the pixel numbers of leaf derived from image analysis can substitute for manual morphology measurements and be suitable for seagrass leaf biomass estimation in future seagrass investigations. Compared with the traditional manual measures, image analysis based on the number of pixels may more easily evaluate the morphological data of broken or damaged seagrass blades. It must also be recognized however, that heavy filamentous algae accumulations which grow beyond the boundaries of the seagrass leaf could result in over-estimation of the leaf area.

Correlations of epiphyte imaging metrics with biomass measures (epiphyte pixels *vs.* epiphyte biomass; $R^2 = 0.61$, $P < 0.05$, $n = 1815$) were weaker than for the seagrass metrics when all project data were analyzed collectively. The moderate correlations in the linear relationships between epiphytic imaging metrics and

biomass metrics may be due to seasonal and environmental conditions that might lead to significant variations in the thickness of the epiphyte biofilm. Changes in epiphyte biomass per epiphyte area (pixel) could result from either change in the community composition and/or the growth rate of the epiphytes. Several studies have observed changes in epiphytic assemblages on different host species (Fredriksen et al., 2005; Trautman and Borowitzka, 1999; Michael et al., 2008; Mabrouk et al. 2014). Likewise, when expressing epiphyte accumulation relative to the seagrass host using normalized metrics (epiphyte biomass/seagrass biomass vs epiphyte pixels/total leaf pixels), correlation was only moderate. This suggested effects of environmental factors and non-linear relationships between epiphytes and seagrass, as previously observed (Borum, 1985; Bulthuis and Woelkerling, 1983; Heijs, 1984). Moreover, the image analysis method does not capture the depth of epiphyte growth on the leaf. Epiphyte communities could colonize seagrass blades in an orderly succession with several stages (Corlett and Jones, 2007; Michael et al., 2008). The diverse morphologies of epiphytic assemblages may impact both biomass and imaging measures, and the epiphyte-seagrass dynamic relationship itself. Further exploration of these relationships may reveal new insights that improve the utility of the imaging methods to detect responses to the environment. Another possible solution

could be, based on the observations reported in this paper, to create seasonal spectral libraries and analyze the data based on appropriate seasonal libraries.

5. Conclusion

The presented scanning and image analysis methodology can extract some of the rich information of scanned seagrass images, including metrics related to seagrass morphology, epiphyte coverage pattern, and potential classification of epiphytic taxa. This provides an informative and readily accessible tool to explore and facilitate better understanding of the complex epiphyte-seagrass relationships. In addition, the images can be archived and shared for future analyses by the community of researchers. Currently, the major challenge of image analysis is related to misclassification and omission of green algal epiphyte groups that resemble the seagrass leaf spectrally. Appropriate spectral profile training to encompass more diverse epiphyte groups which may present on a seasonal basis or under unique environmental conditions may be necessary. Object recognition and implementation of thresholds, texture and edge detection should also improve classification and detection of object boundaries as well as other spatially defining features of seagrass and epiphyte

types within the images. More recent deep learning methods present themselves as additional tools to improve classification results (Mehrubeoglu et al., 2021) and image processing efficiency (Aoki et al., 2022) but require more data sets for successful training and classification.

Funding

The experiment and production of this manuscript was supported by the Texas A&M University-Corpus Christi (TAMU-CC) Research & Innovation Awards (C.H. and K.C.), TAMU-CC Research Enhancement Award (K.C.), and Millicent Quammen Memorial Research Award to C.H. (Center for Coastal Studies, TAMU-CC).

Acknowledgements

The authors thank the ICW RV Park in Aransas Pass, TX for access to the seagrass study site. The authors appreciate equipment support for sampling from Mr. Robert Duke (Center for Coastal Studies, TAMU-CC). The authors thank Dr. Hua Zhang (Department of Engineering, TAMU-CC) for providing (UAV) imagery of the study area. The authors would also like to thank Dr. Ed Proffitt (Department of Life Science, TAMU-CC), Dr. Patrick Larkin (Department of Physical & Environmental Sciences, TAMU-CC), and Dr. Blair Sterbaboatwright (Department of Mathematics and Statistics, TAMU-CC) for critical discussions regarding statistical analysis.

Data availability

The authors confirm that the data supporting the findings of this study are available within the article. Raw data of this study are available from the corresponding author KC and first author CH, upon reasonable request.

References:

Ahrens, N., Grubbs, F., 2012. A western range extension for *Caprella scaura* (Amphipoda: Caprellidae) in the Aransas Bay Ecosystem, Texas. Gulf and Caribbean Research 24, 7–11.

https://doi.org/10.18785/gcr.2401.02

Albis-Salas, M.R., Gavio, B., 2011. Notes on marine algae in the International Biosphere Reserve Seaflower, Caribbean Colombian I: new records of macroalgal epiphytes on the seagrass *Thalassia testudinum*. Botanica Marina 54, 537–543. https://doi.org/10.1515/BOT.2011.069

Aoki, L.R., Rappazzo, B., Beatty, D.S., Domke, L.K., Eckert, G.L., Eisenlord, M.E., Graham, O.J., Harper, L., Hawthorne, T.L., Hessing-Lewis, M., Hovel, K.A., Monteith, Z.L., Mueller, R.S., Olson, A.M., Prentice, C., Stachowicz, J.J., Tomas, F., Yang, B., Duffy, J.E., Gomes, C., Harvell, C.D., 2022. Disease surveillance by artificial intelligence links eelgrass wasting disease to ocean warming across latitudes. Limnology and Oceanography 67, 1577–1589. https://doi.org/10.1002/lno.12152

Armitage, A.R., Frankovich, T.A., Fourqurean, J.W., 2006. Variable responses within epiphytic and benthic microalgal communities to nutrient enrichment. Hydrobiologia 569, 423–435. https://doi.org/10.1515/BOT.2011.069

Aumack, C.F., Amsler, C.D., McClintock, J.B., Baker, B.J., 2011.

Impacts of mesograzers on epiphyte and endophyte growth associated with chemically defended macroalge from the Western Antarctic Peninsula: A mesocosm experiment. Journal of Phycology 47, 36–41. https://doi.org/10.1111/j.1529-8817.2010.00927.x

Bankar, S., Dube, A., Kadam, P., Deokule, S., 2014. Plant disease detection techniques using Canny Edge Detection & Color Histogram in Image Processing. International Journal of Computer Science and Information Technologies 5(2), 1165-1169. ISSN: 0975-9646 https://citeseerx.ist.psu.edu/document?repid=rep1&type=pdf&doi=5c58125494432dfa1f9c8c9e8f0d82282cbd2664 (Accessed 16 August 2023)

Boese, B.L., Clinton, P.J., Dennis, D., Golden, R.C., Kim, B., 2008. Digital image analysis of *Zostera marina* leaf injury. Aquatic Botany 88, 87–90. https://doi.org/10.1016/j.aquabot.2007.08.016

Borowitzka, M.A., Lavery, P.S., van Keulen, M., 2007. Epiphytes of Seagrasses, in: Larkum, A.W.D., Orth, R.J., Duarte, C.M. (Eds.), Seagrasses: Biology, Ecology and Conservation. Springer

Netherlands, Dordrecht, pp. 441–461.

Borum, J., 1985. Development of epiphytic communities on eelgrass (*Zostera marina*) along a nutrient gradient in a Danish estuary. Marine Biology 87(2), 211–218. https://doi.org/10.1007/BF00539431

Brodersen, K.E., Lichtenberg, M., Paz, L.C., Kühl, M., 2015. Epiphyte-cover on seagrass (*Zostera marina* L.) leaves impedes plant performance and radial O_2 loss from the below-ground tissue. Frontiers in Marine Science 2, Article 58. https://doi.org/10.3389/fmars.2015.00058

Bulthuis, D.A., Woelkerling, W.J., 1983. Biomass accumulation and shading effects of epiphytes on leaves of the seagrass, *Heterozostera tasmanica*, in Victoria, Australia. Aquatic Botany 16, 137–148. https://doi.org/10.1016/0304-3770(83)90089-X

Burkholder, J.M., Tomasko, D.A., Touchette, B.W., 2007. Seagrasses and eutrophication. Journal of Experimental Marine Biology and Ecology 350(1-2), 46–72. https://doi.org/10.1016/j.jembe.2007.06.024

1117 Campbell, J.E., Fourqurean, J.W., 2014. Ocean acidification
1118 outweighs nutrient effects in structuring seagrass epiphyte
1119 communities. Journal of Ecology 102(3), 730–737.
1120 https://doi.org/10.1111/1365-2745.12233
1121
1122 Canny, J., 1986. A computational approach to edge detection.
1123 *IEEE* Transactions on Pattern Analysis and Machine Intelligence
1124 6, 679–698. https://doi.org/10.1109/TPAMI.1986.4767851
1125
1126 Canonico, G., Buttigieg, P.L., Montes, E., Muller-Karger, F.E.,
1127 Stepien, C., Wright, D., Benson, A., Helmuth, B., Costello, M.,
1128 Sousa-Pinto, I., Saeedi, H., Newton, J., Appeltans, W., Bednaršek,
1129 N., Bodrossy, L., Best, B.D., Brandt, A., Goodwin, K.D., Iken, K.,
1130 Marques, A.C., Miloslavich, P., Ostrowski, M., Turner, W.,
1131 Achterberg, E.P., Barry, T., Defeo, O., Bigatti, G., Henry, L.-A.,
1132 Ramiro-Sánchez, B., Durán, P., Morato, T., Roberts, J.M., García-
1133 Alegre, A., Cuadrado, M.S., Murton, B., 2019. Global
1134 observational needs and resources for marine biodiversity.
1135 Frontiers in Marine Science 6, Article 367.
1136 https://doi.org/10.3389/fmars.2019.00367
1137
1138 Canty, M.J., 2014. Image Analysis, Classification and Change
1139 Detection in Remote Sensing: With Algorithms for ENVI/IDL and

Python, Third Edition. CRC Press., Boca Raton, FL.

Codizar, A.L., Solano, G., 2016. Plant leaf recognition by venation and shape using artificial neural networks, in: 2016 7th International Conference on Information, Intelligence, Systems Applications (IISA), pp. 1–4. IEEE. https://doi.org/10.1109/IISA.2016.7785361

Congdon, V.M., Dunton, K.H., 2016. A Long-term Seagrass Monitoring Program for Corpus Christi Bay and Upper Laguna Madre. Draft Report Contract No. 1510. Coastal Bend Bay & Estuaries Program, pp. 1-27. https://www.cbbep.org/manager/wp-content/uploads/1610-Final-Report-CBBEP.pdf (Accessed 18 August 2023)

Corlett, H., Jones, B., 2007. Epiphyte communities on *Thalassia testudinum* from Grand Cayman, British West Indies: Their composition, structure, and contribution to lagoonal sediments. Sedimentary Geology 194(3-4), 245–262. https://doi.org/10.1016/j.sedgeo.2006.06.010

Cornelisen, C.D., Thomas, F.I.M., 2004. Ammonium and nitrate uptake by leaves of the seagrass *Thalassia testudinum*: impact of

hydrodynamic regime and epiphyte cover on uptake rates. Journal of Marine Systems 49(1-4), 177–194. https://doi.org/10.1016/j.jmarsys.2003.05.008

Crump, B.C., Wojahn, J.M., Tomas, F., Mueller, R.S., 2018. Metatranscriptomics and amplicon sequencing reveal mutualisms in seagrass microbiomes. Frontiers in Microbiology 9, Article 388. https://doi.org/10.3389/fmicb.2018.00388

Dennison, W.C., Alberte, R.S., 1985. Role of daily light period in the depth distribution of *Zostera marina* (eelgrass). Marine Ecology Progress Series 25, 51-61. https://doi.org/10.1016/0022-0981(86)90217-0

Dennison, W.C., Alberte, R.S., 1986. Photoadaptation and growth of *Zostera marina* L. (eelgrass) transplants along a depth gradient. Journal of Experimental Marine Biology and Ecology 98(3), 265–282. https://doi.org/10.3354/meps025051

Dennison, W.C., Orth, R.J., Moore, K.A., Stevenson, J.C., Carter, V., Kollar, S., Bergstrom, P.W., Batiuk, R.A., 1993. Assessing water quality with submersed aquatic vegetation. BioScience 43(2), 86–94. https://doi.org/10.2307/1311969

Diaz-Pulido, G., Díaz-Ruíz, M., 2003. Diversity of benthic marine algae of the Colombian Atlantic. Biota Colombiana 4(2), 203-246. http://www.Redalyc.org/articulo.oa?id=49140206

Dirnberger, J.M., 1990. Benthic determinants of settlement for planktonic larvae: availability of settlement sites for the tube-building polychaeta *Spirorbis spirillum* (Linnaeus) settling onto seagrass blades. Journal of Experimental Marine Biology and Ecology 140(1-2), 89–105. https://doi.org/10.1016/0022-0981(90)90084-P

Duffy, J.E. 2006. Biodiversity and the functioning of seagrass ecosystems. Marine Ecology Progress Series Vol. 311: 233–250.

Dunton, K., Pulich, W., Mutchler, T., 2010. A seagrass monitoring program for Texas coastal waters. Final Report Contract No. 0627. Coastal Bend Bays & Estuaries Program, pp. 1-39. https://www.cbbep.org/manager/wp-content/uploads/1429-Seagrass-Monitoring-Final-Report.pdf (Accessed 18 August 2023)

Durako, M.J., Howarth, J.F., 2017. Leaf spectral reflectance shows *Thalassia testudinum* seedlings more sensitive to hypersalinity

than hyposalinity. Frontiers in Plant Science 8, Article 1127. https://doi.org/10.3389/fpls.2017.01127

Fong, P., Harwell, M.A., 1994. Modeling seagrass communities in tropical and subtropical bays and estuaries: a mathematical model synthesis of current hypotheses. Bulletin of Marine Science 54(3), 757–781.

Frankovich, T.A., Armitage, A.R., Wachnicka, A.H., Gaiser, E.E., Fourqurean, J.W., 2009. Nutrient effects on seagrass epiphyte community structure in Florida Bay. Journal of Phycology 45(5), 1010-1020. https://doi.org/10.1111/j.1529-8817.2009.00745.x

Frankovich, T.A., Fourqurean, J.W., 1997. Seagrass epiphyte loads along a nutrient availability gradient, Florida Bay, USA. Marine Ecology Progress Series 159, 37–50. https://doi.org/10.3354/meps159037

Fredriksen, S., Christie, H., Andre Sæthre, B., 2005. Species richness in macroalgae and macrofauna assemblages on *Fucus serratus* L. (Phaeophyceae) and *Zostera marina* L. (Angiospermae) in Skagerrak, Norway. Marine Biology Research 1(1), 2–19. https://doi.org/10.1080/17451000510018953

Giovannetti, E., Montefalcone, M., Morri, C., Bianchi, C.N., Albertelli, G., 2010. Early warning response of *Posidonia oceanica* epiphyte community to environmental alterations (Ligurian Sea, NW Mediterranean). Marine Pollution Bulletin 60(7), 1031–1039. https://doi.org/10.1016/j.marpolbul.2010.01.024

Golzarian, M.R., Frick, R.A., Rajendran, K., Berger, B., Roy, S., Tester, M., Lun, D.S., 2011. Accurate inference of shoot biomass from high-throughput images of cereal plants. Plant Methods 7(1), 1-11. https://doi.org/10.1186/1746-4811-7-2

Greiner, J.T., McGlathery, K.J., Gunnell, J., McKee, B.A., 2013. Seagrass restoration enhances "blue carbon" sequestration in coastal waters. PLOS ONE 8(8): e72469. https://doi.org/10.1371/journal.pone.0072469

Harlin, M.M., 1975. Epiphyte—host relations in seagrass communities. Aquatic Botany 1, 125–131. https://doi.org/10.1016/0304-3770(75)90017-0

Harlin, M.M., 1973. Transfer of products between epiphytic marine algae and host plants. Journal of Phycology 9(3), 243–248.

https://doi.org/10.1111/j.1529-8817.1973.tb04088.x

Heck, K.L., Nadeau, D.A., Thomas, R., 1997. The nursery role of seagrass beds. Gulf of Mexico Science 15(1), Article 8. https://doi.org/10.18785/goms.1501.08

Heck, K.L., Valentine, J.F., 2007. The primacy of top-down effects in shallow benthic ecosystems. Estuaries and Coasts 30(3), 371–381. https://doi.org/10.1007/BF02819384

Heck, K.L., Valentine, J.F., 2006. Plant–herbivore interactions in seagrass meadows. Journal of Experimental Marine Biology and Ecology 330(1), 420–436. https://doi.org/10.1016/j.jembe.2005.12.044

Heck K.L. Jr, Hays C., Orth R.J. 2003. Critical evaluation of the nursery role hypothesis for seagrass meadows. Marine Ecology Progress Series 253:123–136.

Hemminga M.A., Duarte C.M. 2000. Seagrass ecology. Cambridge University Press, New York, 298 pp. https://dx.doi.org/10.1017/CBO9780511525551

Heijs, F.M.L., 1984. Annual biomass and production of epiphytes in three monospecific seagrass communities of *Thalassia hemprichii* (Ehrenb.) Aschers. Aquatic Botany 20(3-4), 195–218. https://doi.org/10.1016/0304-3770(84)90087-1

Hickman, M., 1971. The standing crop and primary productivity of the epiphyton attached to *Equisetum fluviatile* L. in Priddy Pool, North Somerset. British Phycological Journal 6(1), 51–59 https://doi.org/10.1080/00071617100650061

Hobson, C., Whisenant, A., 2018. Seagrass monitoring in San Antonio Bay, Texas with implications for management. Texas Journal of Science 70(1), Article 1. https://doi.org/10.32011/txjsci_70_1_Article1

Huang, C., Piñón, C., Mehrubeoglu, M., Cammarata, K., 2023. Image analysis reveals environmental influences on the seagrass-epiphyte dynamic relationship for *Thalassia testudinum* in the northwestern Gulf of Mexico. Frontiers in Marine Science 9. https://doi.org/10.3389/fmars.2022.1096307

Van Katwijk, M.M., Thorhaug, A., Marbà, N., Orth, R.J., Duarte, C.M., Kendrick, G.A., Althuizen, I.H.J., Balestri, E., Bernard, G.,

Cambridge, M.L., Cunha, A., Durance, C., Giesen, W., Han, Q., Hosokawa, S., Kiswara, W., Komatsu, T., Lardicci, C., Lee, K.-S., Meinesz, A., Nakaoka, M., O'Brien, K.R., Paling, E.I., Pickerell, C., Ransijn, A.M.A., Verduin, J.J., 2016. Global analysis of seagrass restoration: the importance of large-scale planting. Journal of Applied Ecology 53(2), 567–578. https://doi.org/10.1111/1365-2664.12562

Kendrick, G.A., Burt, J.S., 1997. Seasonal changes in epiphytic macro-algae assemblages between offshore exposed and inshore protected *Posidonia sinuosa* Cambridge et Kuo seagrass meadows, Western Australia. Botanica Marina 40(1-6), 77–86. https://doi.org/10.1515/botm.1997.40.1-6.77

Kitting, C.L., Fry, B., Morgan, M.D., 1984. Detection of inconspicuous epiphytic algae supporting food webs in seagrass meadows. Oecologia 62(2), 145–149. https://doi.org/10.1007/BF00379006

Kruse, F.A., Lefkoff, A.B., Boardman, J.W., Heidebrecht, K.B., Shapiro, A.T., Barloon, P.J., Goetz, A.F.H., 1993. The spectral image processing system (SIPS)—interactive visualization and analysis of imaging spectrometer data. Remote Sensing of

Environment 44(2-3), 145–163. https://doi.org/10.1016/0034-4257(93)90013-N

Lavery, P.S., Vanderklift, M.A., 2002. A comparison of spatial and temporal patterns in epiphytic macroalgal assemblages of the seagrasses *Amphibolis griffithii* and *Posidonia coriacea*. Marine Ecology Progress Series 236, 99–112. https://doi.org/10.3354/meps236099

Lyons, M., Phinn, S., Roelfsema, C., 2011. Integrating Quickbird multi-spectral satellite and field data: Mapping bathymetry, seagrass cover, seagrass species and change in Moreton Bay, Australia in 2004 and 2007. Remote Sensing 3(1), 42–64. https://doi.org/10.3390/rs3010042

Mabrouk, L., Brahim, M.B., Hamza, A., and Bradai, M.-N. 2014. Diversity and temporal fluctuations of epiphytes and sessile invertebrates on the rhizomes of *Posidonia oceanica* in a seagrass meadow off Tunisia. Marine Ecology 35, 212-220.

McMahon, K., Collier, C., Lavery, P.S., 2013. Identifying robust bioindicators of light stress in seagrasses: a meta-analysis. Ecological Indicators 30, 7–15.

https://doi.org/10.1016/j.ecolind.2013.01.030

Mehrubeoglu, M., Vargas, I., Huang, C., Cammarata, K., 2021. Segmentation of seagrass blade images using deep learning, in: Real-Time Image Processing and Deep Learning 2021 (Vol. 11736, p. 1173605). International Society for Optics and Photonics. https://doi.org/10.1117/12.2587057

Michael, T.S., Shin, H.W., Hanna, R., Spafford, D.C., 2008. A review of epiphyte community development: surface interactions and settlement on seagrass. Journal of Environmental Biology 29(4) 629-638. PMID: 19195408

Minnery, G.A., Rezak, R., Bright, T.J., 1985. Depth zonation and growth form of crustose coralline algae: Flower Garden Banks, Northwestern Gulf of Mexico, in: Toomey, D.F., Nitecki, M.H. (Eds.), Paleoalgology. Springer, Berlin, Heidelberg, pp. 237–246. https://doi.org/10.1007/978-3-642-70355-3_18

Moncreiff, C., Sullivan, M., Daehnick, A., 1992. Primary production dynamics in seagrass beds of Mississippi Sound: the contributions of seagrass epiphytic algae, sand microflora, and phytoplankton. Marine Ecology Progress Series 87, 161–171.

https://doi.org/10.3354/meps087161

Morgan, M.D., Kitting, C.L., 1984. Productivity and utilization of the seagrass *Halodule wrightii* and its attached epiphytes. Limnology and Oceanography 29(5), 1066–1076. https://doi.org/10.4319/lo.1984.29.5.1066

Neckles, H.A., Kopp, B.S., Peterson, B.J., Pooler, P.S., 2012. Integrating scales of seagrass monitoring to meet conservation needs. Estuaries and Coasts 35(1), 23–46. https://doi.org/10.1007/s12237-011-9410-x

Nelson, T.A., Waaland, J.R., 1997. Seasonality of eelgrass, epiphyte, and grazer biomass and productivity in subtidal eelgrass meadows subjected to moderate tidal amplitude. Aquatic Botany 56, 51–74. https://doi.org/10.1016/S0304-3770(96)01094-7

Nelson, W.G., 2017a. Patterns of shading tolerance determined from experimental light reduction studies of seagrasses. Aquatic Botany 141, 39–46. https://doi.org/10.1016/j.aquabot.2017.05.002

Nelson, W.G., 2017b. Development of an epiphyte indicator of nutrient enrichment: threshold values for seagrass epiphyte load.

Ecological Indicators 74, 343–356. https://doi.org/10.1016/j.ecolind.2016.11.035

Nielsen, J., Lethbridge, R., 1989. Feeding and the epiphyte food resources of gastropods living on leaves of the Seagrass *Amphibolis griffithii* in south-western Australia. Journal of the Malacological Society of Australia 10(1), 47–58. https://doi.org/10.1080/00852988.1989.10674005

Nieuwenhuize, J., Erftemeijer, P.L.A., Maas, Y.E.M., Verwaal, M., Nienhuis, P.H., 1994. Pretreatment artefacts associated with the removal of calcareous epiphytes from seagrass leaves. Aquatic Botany 48(3-4), 355–361. https://doi.org/10.1016/0304-3770(94)90026-4

Novak, A.B., Short, F.T., 2011. Leaf reddening in the seagrass *Thalassia testudinum* in relation to anthocyanins, seagrass physiology and morphology, and plant protection. Marine Biology 158(6), 1403–1416. https://doi.org/10.1007/s00227-011-1658-y

Orth, R.J., Carruthers, T.J.B., Dennison, W.C., Duarte, C.M., Fourqurean, J.W., Heck, K.L., Hughes, A.R., Kendrick, G.A., Kenworthy, W.J., Olyarnik, S., Short, F.T., Waycott, M., Williams,

S.L., 2006. A Global Crisis for Seagrass Ecosystems. BioScience 56(12), 987–996. https://doi.org/10.1641/0006-3568(2006)56[987:AGCFSE]2.0.CO;2

Orth, R.J., Van Montfrans, J., 1984. Epiphyte-seagrass relationships with an emphasis on the role of micrograzing: a review. Aquatic Botany 18(1-2), 43–69. https://doi.org/10.1016/0304-3770(84)90080-9

Ow, Y.X., Ng, K.J., Lai, S., Yaakub, S.M., Todd, P., 2020. Contribution of epiphyte load to light attenuation on seagrass leaves is small but critical in turbid waters. Marine and Freshwater Research 71(8), 929–934. https://doi.org/10.1071/MF19178

Papazian, S., Parrot, D., Burýšková, B., Weinberger, F., Tasdemir, D., 2019. Surface chemical defence of the eelgrass *Zostera marina* against microbial foulers. Scientific Reports 9, Article number: 3323. https://doi.org/10.1038/s41598-019-39212-3

Penhale, P.A., 1977. Macrophyte-epiphyte biomass and productivity in an eelgrass (*Zostera marina* L.) community. Journal of Experimental Marine Biology and Ecology 26(2), 211–224. https://doi.org/10.1016/0022-0981(77)90109-5

Peterson, B.J., Frankovich, T.A., Zieman, J.C., 2007. Response of seagrass epiphyte loading to field manipulations of fertilization, gastropod grazing and leaf turnover rates. Journal of Experimental Marine Biology and Ecology 349(1), 61–72. https://doi.org/10.1016/j.jembe.2007.04.012

Pinckney, J.L., Micheli, F., 1998. Microalgae on seagrass mimics: Does epiphyte community structure differ from live seagrasses? Journal of Experimental Marine Biology and Ecology 221(1), 59–70. https://doi.org/10.1016/S0022-0981(97)00115-9

Ralph, P.J., Durako, M.J., Enríquez, S., Collier, C.J., Doblin, M.A., 2007. Impact of light limitation on seagrasses. Journal of Experimental Marine Biology and Ecology 350(1-2), 176–193. https://doi.org/10.1016/j.jembe.2007.06.017

Reyes, J., Sansón, M., 1997. Temporal distribution and reproductive phenology of the epiphytes on *Cymodocea nodosa* leaves in the Canary Islands. Botanica Marina 40(1-6), 193–201. https://doi.org/10.1515/botm.1997.40.1-6.193

Salman, A., Semwal, A., Bhatt, U., Thakkar, V.M., 2017. Leaf

1462 classification and identification using Canny Edge Detector and
1463 SVM classifier, in: 2017 International Conference on Inventive
1464 Systems and Control (ICISC), pp. 1–4. IEEE.
1465 https://doi.org/10.1109/ICISC.2017.8068597
1466
1467 Sand-Jensen, K.A.J., 1977. Effect of epiphytes on eelgrass
1468 photosynthesis. Aquatic Botany 3, 55–63.
1469 https://doi.org/10.1016/0304-3770(77)90004-3
1470
1471 Schindelin, J., Arganda-Carreras, I., Frise, E., Kaynig, V., Longair,
1472 M., Pietzsch, T., Preibisch, S., Rueden, C., Saalfeld, S., Schmid,
1473 B., 2012. Fiji: an open-source platform for biological-image
1474 analysis. Nature methods 9, 676–682.
1475 https://doi.org/10.1038/nmeth.2019
1476
1477 Schneider, C.A., Rasband, W.S., Eliceiri, K.W., 2012. NIH Image
1478 to ImageJ: 25 years of image analysis. Nature methods 9, 671–675.
1479 https://doi.org/10.1038/nmeth.2089
1480
1481 Shamir, L., Delaney, J.D., Orlov, N., Eckley, D.M., Goldberg, I.G.,
1482 2010. Pattern Recognition Software and Techniques for Biological
1483 Image Analysis. PLOS Computational Biology 6(11): e1000974.
1484 https://doi.org/10.1371/journal.pcbi.1000974

Thorhaug, A., Richardson, A.D., Berlyn, G.P., 2006. Spectral reflectance of *Thalassia testudinum* (Hydrocharitaceae) seagrass: low salinity effects. American Journal of Botany 93(1), 110–117. https://doi.org/10.3732/ajb.93.1.110

Trautman, D., and Borowitzka, M. 1999. Distribution of the epiphytic organisms on *Posidonia australis* and *P. sinuosa*, two seagrasses with differing leaf morphology. Marine Ecology Progress Series. 179, 215-229. https://doi.org/10.3354/meps179215

Whalen, M.A., Duffy, J.E., Grace, J.B., 2013. Temporal shifts in top-down vs. bottom-up control of epiphytic algae in a seagrass ecosystem. Ecology 94(2), 510–520. https://doi.org/10.1890/12-0156.1

Wynne, M.J, 2008. A Checklist of Benthic Marine Algae of the Coast of Texas. Gulf of Mexico Science 26(1) Article 7. https://doi.org/10.18785/goms.2601.07

Yuhas, R.H., Goetz, A.F.H., Boardman, J.W., 1992. Discrimination among semi-arid landscape endmembers using the

Spectral Angle Mapper (SAM) algorithm, in: JPL, Summaries of the Third Annual JPL Airborne Geoscience Workshop. Volume 1: AVIRS Workshop. https://ntrs.nasa.gov/citations/19940012238 (Accessed 18 August 2023)

Zimba, P.V., Hopson, M.S., 1997. Quantification of epiphyte removal efficiency from submersed aquatic plants. Aquatic Botany 58(2), 173–179. https://doi.org/10.1016/S0304-3770(97)00002-8